ACS Catalysis

pubs.acs.org/acscatalysis Research Article

Heterogeneous Iridium-Catalyzed Carbene N−H Bond Insertion with α-Alkyl Diazo Esters

Ping Guo,[#] Yan Chen,[#] Lei Tao,[#] Shufang Ji,[#] Ruixue Zhang, Zedong Zhang, Xiao Liang, Dingsheng Wang,* Yadong Li,* and Jie Zhao*

Cite This: ACS Catal. 2024, 14, 4690−4698 Read Online

ACCESS | Metrics & More | Article Recommendations | Supporting Information

ABSTRACT: A heterogeneous iridium single-atom site catalyst (Ir-SA) was synthesized and investigated in catalyzing the carbene insertion reaction with challenging α-alkyl diazo ester substrates. With only 0.23 mol % catalyst loading, our Ir-SA demonstrated remarkable performance in heterogeneous carbene N−H bond insertion reactions involving various (hetero) aryl amines coupled with α-alkyl diazo esters. Notably, in the case of using a chiral diamino substrate with two reactive sites, Ir-SA exhibited high selectivity toward single carbene N−H insertion, leading to the generation of a class of unsymmetric chiral diamino ligands. Further mechanism study revealed that the lower activation barrier associated with the single N−H bond insertion step, as compared to either β-hydride elimination or downstream dual N−H bond insertion, accounted for the remarkable selectivity observed in this carbene insertion reaction catalyzed by Ir-SA.

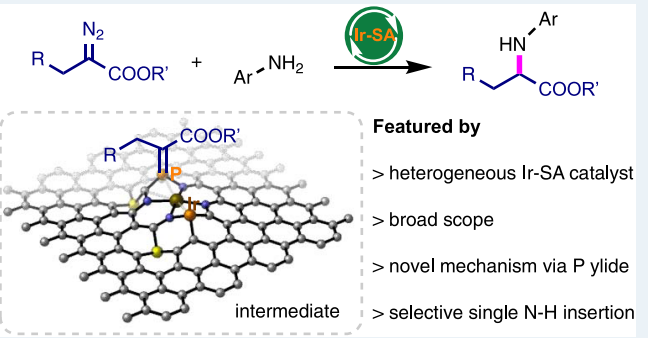

KEYWORDS: *heterogeneous, carbene insertion, iridium, selectivity, catalysis.*

Heterogeneous catalysts with well-defined structures have been proven to exhibit excellent reactivity, high selectivity, and substantial turnover numbers in numerous important organic transformations.[1−8] Notably, the utilization of heterogeneous catalysis has been extensively explored in Suzuki−Miyaura cross couplings[9−12] selective addition of unsaturated compounds,[13−19] alkylation reaction,[20−25] hydrogenation, and oxidation.[26−29] These investigations highlight the potential of this new class of heterogeneous homogeneous catalytic systems. Single-atom site catalysts (SACs) stand out due to their characteristic structures, achieved through precise control during preparation.[30−36] Different preparative conditions would affect the chemical properties of SACs, including their oxidant state, the coordinating structure, as well as the chemical environments. The resulting diversity in the structure serves as an effective means to significantly boost catalytic performance in the sense of activity and selectivity. The ability to finely tailor these catalysts at the atomic level opens an avenue for the development of heterogeneous catalytic organic transformations.[37,38] Previously, we have demonstrated a single-atom site Ir catalyst being effective for selective carbene O−H insertion, while the substrates feature multiple nucleophilic reactive sites.[60] Importantly, the origin of selectivity was addressed by the fact of the lower oxidative state of the Ir atom relative to that of analogous homogeneous IrCO(TTP)Cl, thereby reducing the electrophilicity of the generated metal carbene. In the alternative, a seminal example reported by Zhang et al. showcased an efficient additive-free hydroboration of alkenes/alkynes catalyzed by Cu SACs. In this case, enhanced activity can be obtained by tuning the polarity of the Cu−O bond on the ceria support.[39] Additionally, capitalizing on the strong electronic metal−support interaction could also be essential. For instance, Li et al. successfully demonstrated the control of regioselectivity in the hydroboration of alkynes using the TiC-supported Cu catalyst.[40] Therefore, SACs have proven to be an efficient and potential class of catalysts, offering promising solutions to address the challenges of reactivity and selectivity in organic synthesis.

Transition-metal-catalyzed carbene insertion into N−H bonds has emerged as a robust method for constructing C−N bonds, enabling the synthesis of diverse nitrogen-containing bioactive compounds and pharmaceuticals.[41−50] While numerous successful examples exist, the exploration of α-alkyl diazo esters as carbene precursors remains limited (Scheme 1). The competitive β-hydride elimination pathway often hinders the desired reactions under homogeneous conditions, resulting in

Received: November 20, 2023
Revised: January 25, 2024
Accepted: February 26, 2024
Published: March 13, 2024

https://doi.org/10.1021/acscatal.3c05635
ACS Catal. 2024, 14, 4690−4698

Scheme 1. Background of Carbene N−H Insertion with α-Alkyl Diazo Ester

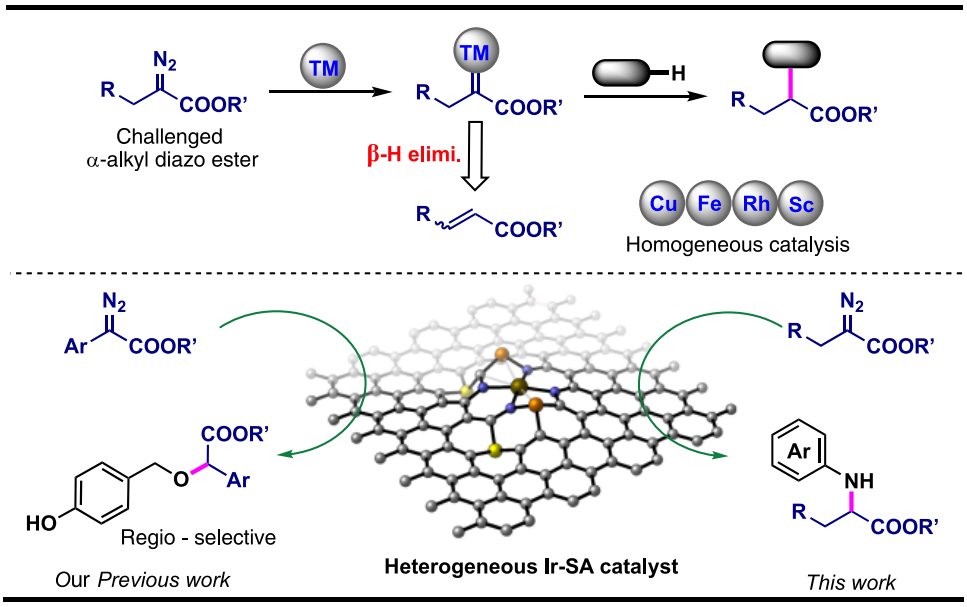

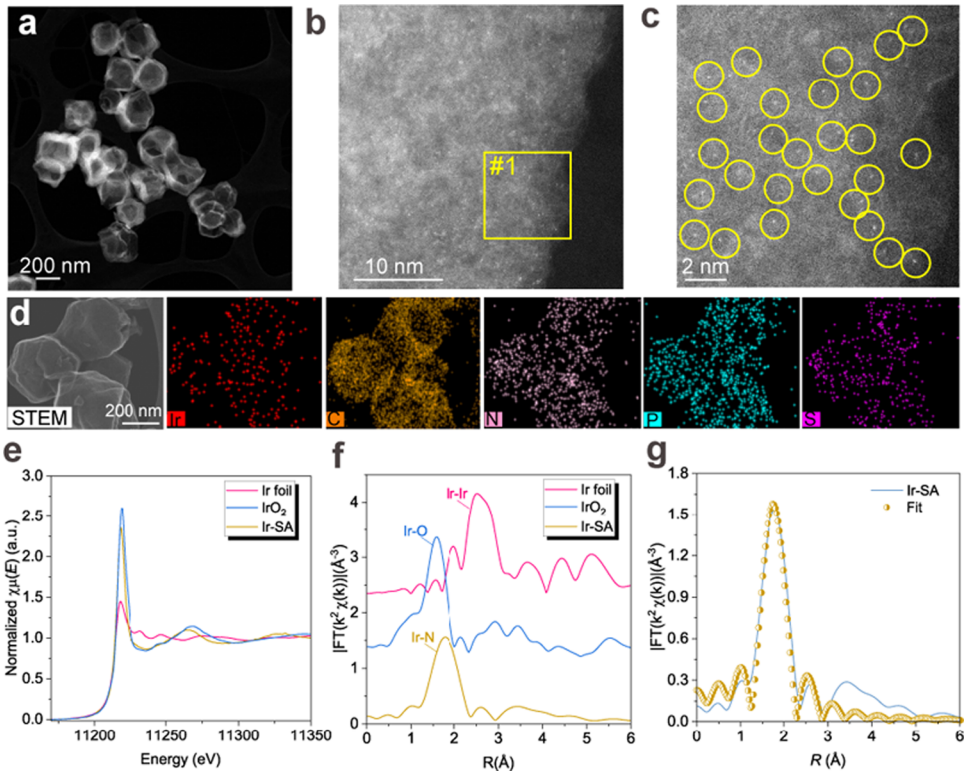

Figure 1. Structural characterizations of Ir-SA. (a) HAADF-STEM image of the Ir-SA catalyst. (b) AC HAADF-STEM image of the Ir-SA catalyst. (c) Enlarged AC HAADF-STEM image of the Ir-SA catalyst. (d) HAADF-STEM image and element maps. (e) Comparison of Ir L3-edge XANES spectra of Ir-SA, Ir foil, and IrO_2 samples. (f) Ir L3-edge k3-weighted FT spectra of the Ir-SA, Ir powder, and IrO_2 samples. (g) Corresponding EXAFS R-space fitting curves. Inset: the schematic model of Ir-SA (Ir, brown; C, gray; N, blue; S, yellow; P, orange).

low yields of the desired products.[51−59] Inspiringly, the Zhou group reported on the strategy using achiral metal complexes combined with chiral phosphoric acids for asymmetric carbene N−H insertion.[57,58] while the Feng group achieved catalytic asymmetric homologation of ketones using α-alkyl diazo esters, with chiral scandium(III) *N,N′*-dioxide as a Lewis acid catalyst.[51−54] These significant research results encouraged us to explore the carbene insertion reaction with this type of a challenged substrate via heterogeneous catalysis.

Recently, we developed a practical preparation method for a heterogeneous iridium single-atom site catalyst (Ir-SA) in which iridium atoms are coordinated with four nitrogen atoms, distributed evenly on a sulfur- and phosphorus-doped carbon support.[60] The primary catalytic study demonstrated that Ir-SA exhibited high reactivity and regioselectivity in carbene

https://doi.org/10.1021/acscatal.3c05635
ACS Catal. 2024, 14, 4690−4698

Table 1. Optimization of Catalysis Conditions[a]

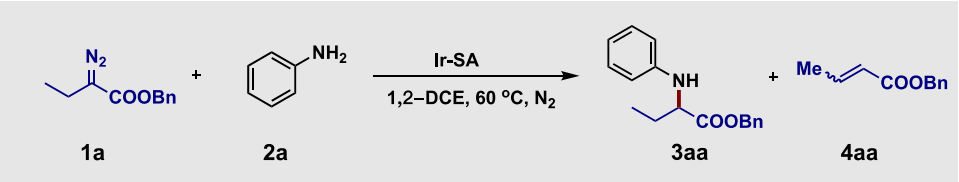

entry	subst. ratio 1a:2a	conc. of 2a (M)	catal. loading (mol %)	yield of 3aa (%)	yield of 4aa (%)
1	1:1	**0.05**	0.46	47	22
2	1:1	**0.1**	0.46	48	17
3	1:1	**0.2**	0.46	63	17
4	1:1	0.2	**0.23**	50	18
5	1.5:1	0.2	0.23	80	45
6[b]	1.5:1	0.2	0.23	7	-
7[c]	1.5:1	0.2	0.23	20	19
8[d]	1.5:1	0.2	0.23	0	0
9[e]	1.5:1	0.2	0.23	0	-

[a]Reaction conditions: diazo ester **1a**, aniline **2a** (0.1 mmol), Ir-SA (4 mg as a catalyst loading of 0.46 mol % or 2 mg as a catalyst loading of 0.23 mol %), 1,2-dichloroethane, and a N_2 atmosphere. The yield of the product was determined by ^{1}H NMR spectra, using 1,3,5-trimethoxylbenzene as the internal standard. [b]Reactions performed under room temperature. [c]Reactions performed in ambient air. [d]Reactions performed with commercial Ir/C catalyst. [e]Reactions performed without catalyst.

insertion into C(sp^3) O−H bonds in the presence of the C(sp^2) O−H bond. Mechanistic investigations indicated that the relatively lower oxidation state of iridium reduced the electrophilicity of the generated metal carbene, facilitating selective insertion into more nucleophilic O−H bonds. Building upon these promising results, we aim to develop a heterogeneous catalytic system for carbene N−H bond insertion reactions with more challenging α-alkyl diazo ester substrates in combination with (hetero) aromatic amines.

PREPARATION OF Ir-SA

The fabrication process and structural confirmation of the Ir-SA catalyst are processed according to the modified version of our developed method.[60] First, iridium(IV) chloride and the monomers of poly(cyclotriphospazene-*co*-4,4′-sulfonyldiphenol) (PZS) were mixed with prepared zeolite imidazolate frameworks-8 (ZIF-8) in methanol. Afterward, trimethylamine (TEA) was added to initiate polymerization to generate ZIF-8/Ir@PZS composites (Figure S1). At last, pyrolysis of the obtained ZIF-8/Ir@PZS at 950 °C under an argon atmosphere led to the desired Ir-SA catalyst.

CHARACTERIZATION OF Ir-SA

As shown in the STEM bright-field image (Figure S2) and STEM secondary electron image (Figure S3), the morphology of the Ir-SA catalyst remains consistently hollow. Moreover, the high-angle annular dark-field scanning TEM (HAADF-STEM) image showed that no obvious iridium nanoparticles were illustrated (Figures 1a and S4), which is further confirmed with the X-ray diffraction pattern (XRD) of Ir-SA (Figures S5). The individual bright dots in Figure 1b and the enlarged image in Figure 1c, marked with yellow circles, are clearly distinguishable from the support. These bright dots indicate the presence of single Ir atoms in Ir-SA without metal agglomeration. The energy-dispersive spectroscopy (EDS) images of Ir-SA confirmed a good dispersion of Ir (in red), C (in orange), N (in pink), P (in blue), and S (in bright purple) elements in the hollow layer (Figures 1d and S4). X-ray photoelectron spectroscopy (XPS) of N, P, and S in Ir-SA was carried out to confirm the binding states and the chemical environment of Ir-SA (Figure S6−S8).

Furthermore, atomic structure analysis of Ir-SA was carried out by a series of X-ray absorption fine structure (XAFS) investigations. First, in the Ir L3-edge X-ray absorption near-edge structure (XANES) curve (Figure 1e), the white-line peak of Ir-SA is located between that of an Ir foil and IrO_2, indicating that the oxidative state of Ir in Ir-SA is positive. Figure 1f shows the comparison of different catalysts on the Fourier transform (FT) extended X-ray absorption fine structure (EXAFS) curve, in which it could be figured out that the maxim peak attributed by Ir−N interaction in Ir-SA is different from peaks contributed by Ir−Ir bonds or Ir−O bonds, implying the existence of Ir atomic sites in Ir-SA. Lastly, the EXAFS fitting curve of Ir-SA is depicted in Figure 1g, in which themaximum peak results from the first shell of Ir−N scattering (more details and fitting parameters are shown Figures S9−S14 and Table S1). Combined with these results and the DFT study, the structure of Ir-SA was confirmed to be four N-ligated Ir single atoms well dispersed on heteroatom-doped carbon support.

CATALYSIS STUDY

To initiate the condition screening for the proposed carbene N−H bond insertion using the heterogeneous Ir-SA catalyst, benzyl 2-diazobutanoate (**1a**) and aniline (**2a**) were chosen as model substrates.

At the outset, the reaction concentration in terms of aniline was optimized, and 0.2 M was found to be the optimal concentration, outperforming 0.1 and 0.05 M (Table 1, entries 1−3). Additionally, reducing the catalyst loading from 0.46 to 0.23 mol % resulted in a slightly lower yield of the desired insertion product (entries 3 and 4). The molar ratio of diazo to aniline also influenced the product yield, with a 1.5:1 ratio demonstrating improved results compared to 1:1 (entries 4 and 5). A significant decrease in the yield was observed when the reaction temperature was lowered to room temperature (entry 6). Performing the reaction under ambient air led to the formation of only 20% of the desired product, indicating the

https://doi.org/10.1021/acscatal.3c05635
ACS Catal. 2024, 14, 4690−4698

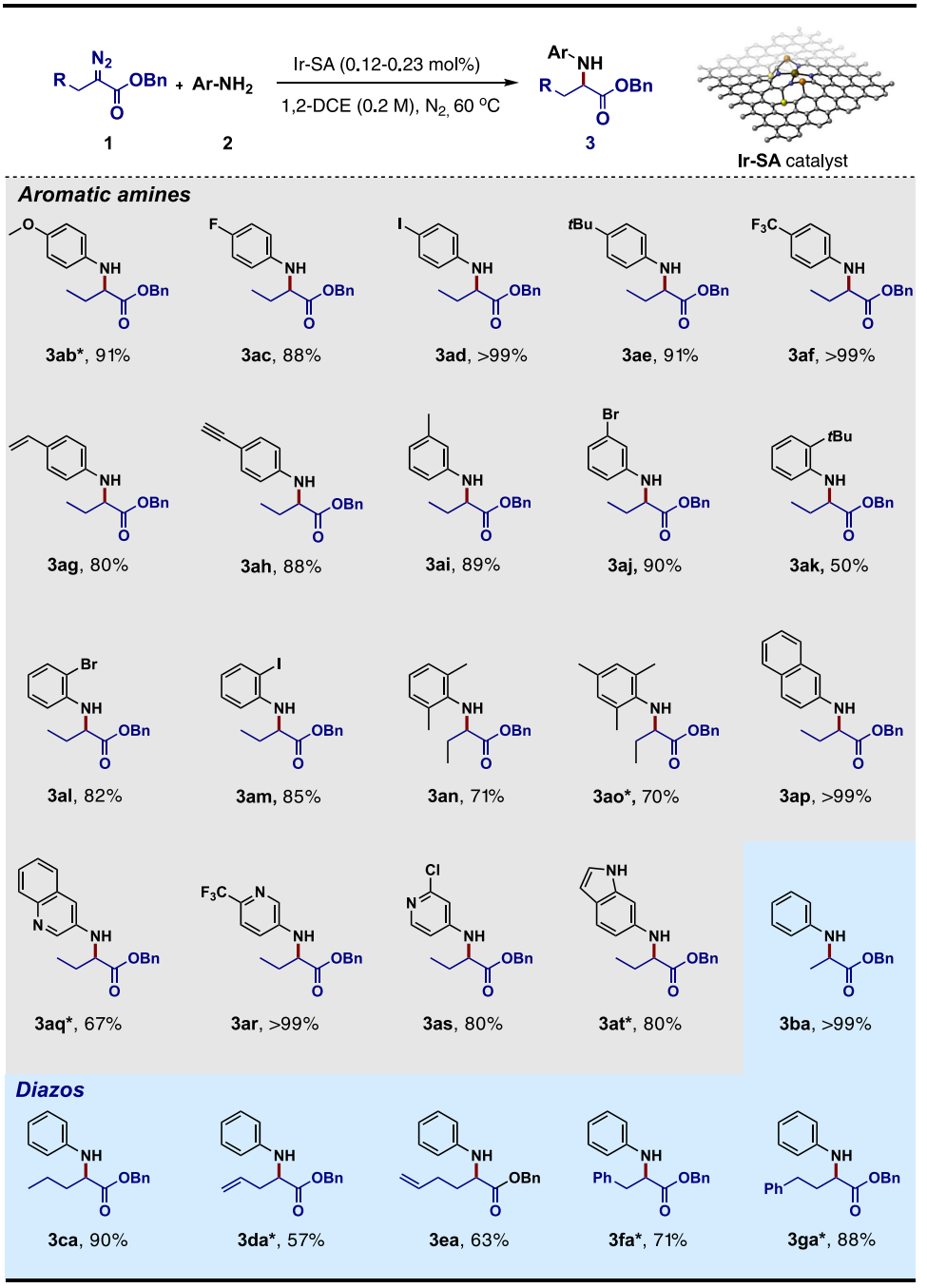

Figure 2. Substrate scope of developed heterogeneous Ir-SA-catalyzed carbene N−H bond insertion. Reaction conditions: diazo esters **1** (0.15 mmol), amine **2** (0.1 mmol), Ir-SA (1 mg, catalyst loading is 0.12 mol %), 1,2-dichloroethane (0.5 mL, 0.2 M), and a N_2 atmosphere. *Ir-SA (2 mg, catalyst loading is 0.23 mol %). The yield of the product was determined by ^{1}H NMR spectra, using 1,3,5-trimethoxylbenzene or 1,3-dinitrobenzene as an internal standard.

requirement of an inert atmosphere (entry 7). Interestingly, a commercial heterogeneous Ir/C catalyst was tested for comparison, but no desired insertion product was observed, indicating the superior potential of Ir-SA with SAC character as an alternative heterogeneous catalyst for industrial applications (entry 8). Moreover, no product was generated in the absence of a catalyst (entry 9). Finally, the optimized conditions for the subsequent substrate scope study were determined as follows: a 1.5:1 molar ratio of diazo to aniline, a 0.2 M concentration of aniline, a 0.23 mol % catalyst loading of Ir-SA, an inert atmosphere, and 1,2-dichloroethane as the solvent. In addition to condition screening, the catalyst-recycling experiments as well as the hot-filtration test have also been performed. The catalyst-recycling results showcase that the yields of reactions decreased after each recycling, while a slight increase in the insertion product was observed after 4 h after hot-filtration (details see SI, Figure S15). These results collectively indicate that the leaching of the catalyst occurred in a very limited amount, similar to observations in our previous work.[60]

With the optimized reaction conditions in hand, we proceeded to investigate the substrate scope of the heterogeneous Ir-SA-catalyzed carbene N−H bond insertion

https://doi.org/10.1021/acscatal.3c05635
ACS Catal. 2024, 14, 4690−4698

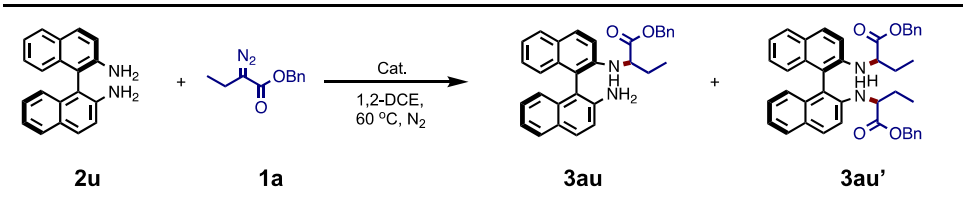

Catalyst	Ir-SA (in use)	Ir-N_4 (w/o S&P)	IrCO(TTP)Cl	Cu_2O	$Cu(OAc)_2$	$Rh(OAc)_2$
Yield of **3au**	81%	31%	52%	41%	27%	16%
Select. of **3au : 3au'**	81 : 19	94 : 6	59 : 41	77 : 23	54 : 46	41 : 59

Figure 3. Comparison of heterogeneous Ir-SA with the most commonly used homogeneous catalysts for carbene N−H insertion of diamine substrate **2u**. Reaction conditions: diazo ester **1a** (0.15 mmol), diamine **2u** (0.1 mmol), catalyst loading (Ir-SA and Ir−N_4 with 0.23 mol %, homogeneous catalysts with 0.2 mol %), 1,2-dichloroethane (0.5 mL, 0.2 M), and a N_2 atmosphere. The yield of the product was determined by ^{1}H NMR spectra, using 1,3,5-trimethoxylbenzene as an internal standard.

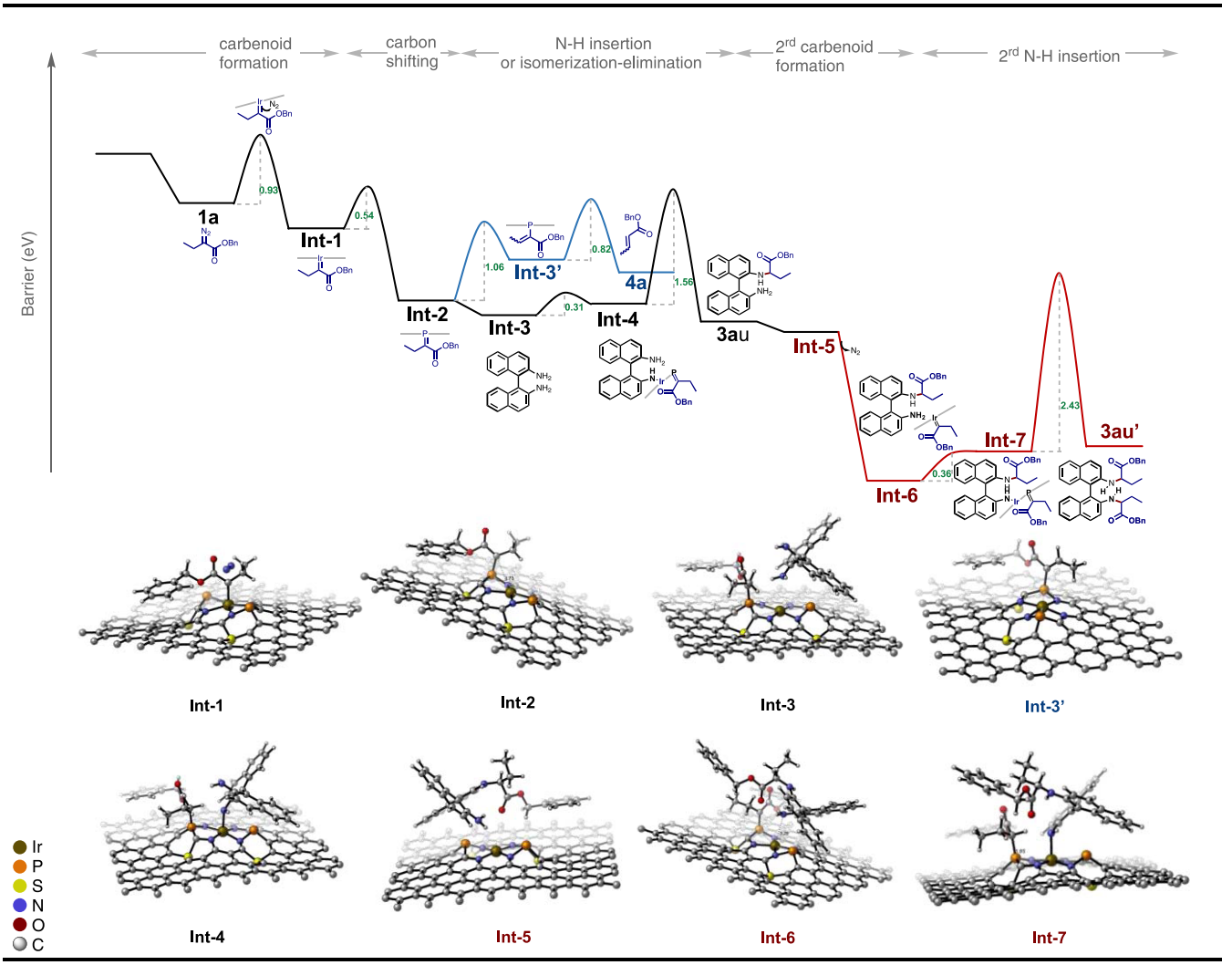

Figure 4. Reaction energy profiles and the structure of intermediates in the DFT study.

(Figure 2). Initially, we examined various aromatic amines, including anilines bearing both electron-donating and electron-withdrawing groups. Anilines with para-substituents such as methoxy, fluoro, iodo, *tert*-butyl, and trifluoro groups reacted

https://doi.org/10.1021/acscatal.3c05635
ACS Catal. 2024, 14, 4690−4698

very efficiently with benzyl 2-diazobutanoate (**3ab**−**3af**, 88 to >99% yield). Notably, substrates containing alkene and alkyne moieties are also adaptable, resulting in the formation of selective N−H insertion products (**3ag**−**3ah**). Moreover, the meta position was found to be flexible, as demonstrated by the successful reactions of 3-methylaniline and 3-bromoaniline under the optimized conditions (**3ai and 3aj**). Interestingly, the ortho-position was observed to be sensitive to steric hindrance, as evidenced by the lower activity of 2-*tert*-butylaniline compared to 2-bromoaniline and 2-iodoaniline (**3ak**−**3am**). Furthermore, both 2,6-dimethylaniline and 2,4,6-trimethylaniline provided moderate yields, indicating the compatibility of this heterogeneous system with multi-substituted anilines (**3an**−**3ao**). Encouragingly, other aromatic and heteroaromatic amines, such as naphthalenyl, quinolinyl, pyridinyl, and indole derivatives, were also amenable to the reaction system (**3ap**−**3at**). Building on these promising results, we further explored various diazo substrates. It was observed that the heterogeneous Ir-SA catalytic system offered moderate to high yields when employing diazo esters composed of methyl, propyl, allyl, but-3-en-1-yl, and benzyl groups (**3ba**−**3ga**).

Encouraged by the broad substrate scope demonstrated by our heterogeneous Ir-SA catalyst, we proceeded to test a more challenging chiral diamine substrate, (*R*)-[1,1′-binaphthalene]-2,2′-diamine (**2u**, (*R*)-BINAM), under the optimized conditions. For the reaction between (*R*)-BINAM and 2-diazobutanoate (**1a**), selectivity on single insertion and double insertion was taken into account for the reaction manner. In parallel, we also examined the structurally similar homogeneous catalyst IrCO(TTP)Cl, as well as copper and rhodium catalysts, which are commonly used in carbene insertion reactions. As shown in Figure 3, the heterogeneous Ir-SA catalyst achieved the highest efficiency for single insertion, leading to the desired production of the monofunctionalized diamine ligand **3au** in an 81% yield (**3au**/**3au**′ = 81:19). We also tested the Ir-SA catalyst without sulfur and phosphorus doping on carbon support (denoted as Ir−N_4, which exhibited a much lower catalytic activity, giving **3au** in a 31% yield. In comparison, IrCO(TTP)Cl exhibited lower activity and poor selectivity, yielding a similar amount of single-insertion product **3au** (52%) and dual-insertion product **3au**′ (36%). Furthermore, Cu_2O, $Cu(OAc)_2$, and $Rh(OAc)_2$ salts all gave **3au** with low efficiency, with yields of 41, 27, and 16%, respectively. These reaction outcomes prompted us to investigate the mechanism and the source of selectivity in the heterogeneous carbene N−H insertion further using density functional theory (DFT) studies.

MECHANISTIC STUDIES

To gain further insights into the carbene N−H bond insertion enabled by our heterogeneous catalyst, we performed subsequent mechanistic investigations using DFT calculations to analyze the energy barriers involved in the reaction between (*R*)-BINAM (**2u**) and 2-diazobutanoate (**1a**) under heterogeneous conditions (Figure 4). The atomic configuration of the Ir-SA catalyst is described in our previous study.[60] The elementary steps, including the formation of a metal carbene (C = Ir) through the decomposition of the diazo ester, the subsequent insertion of the N−H bond into the metal carbene intermediate, and *β*-hydride elimination, were considered to elucidate the selectivity between single N−H bond insertion, dual N−H bond insertion, and alkene formation. Initially, a regular iridium carbene formation step was observed with an activation barrier of 0.93 eV (**Int-1**). Interestingly, we observed an unexpected step where the carbene species shifted from the Ir metal center to the phosphorus atom near the metal, overcoming a small barrier of 0.54 eV. This intermediate, known as the carbon-shifting intermediate (**Int-2**), showed a preference for the single N−H bond insertion step, leading to **3au** (represented by the black curve), rather than the *β*-H elimination step, leading to the alkene side product **4a** (represented by the blue curve). Moreover, the dual-insertion step (represented by the red curve) leading to **3au**′ was disfavored, exhibiting a much higher barrier of 2.43 eV.

Taking all of these steps into consideration, it can be concluded that the N−H carbene insertion employing our heterogeneous Ir-SA catalyst likely proceeds through an inner-sphere mechanism. In this process, the carbene shifts from the carbon atom to the phosphorus atom, generating a phosphorus ylide for subsequent addition by Ir−N species. Furthermore, the achieved high selectivity toward single N−H insertion can be rationalized by the different activation barriers leading to the three possible products.

CONCLUSIONS

The robust heterogeneous iridium single-atom site catalyst (Ir-SA), featuring coordination of four nitrogen atoms distributed on heteroatom (phosphorus and sulfur)-doped carbon, was studied for its catalytic activity in carbene N−H bond insertion reactions using *α*-alkyl diazo esters and (hetero)aromatic amines as reactants. In the scope study, our heterogeneous catalytic system exhibited both high activities, with turnovers up to 7000, and excellent substrate compatibility. Notably, when benzyl 2-diazobutanoate (**1a**) and the chiral diamine substrate (*R*)-BINAM (**2u**) were employed, Ir-SA demonstrated the highest selectivity for single N−H bond insertion, leading to the formation of a novel asymmetric diamine ligand. Mechanistic studies revealed that the relatively lower activation barrier for single N−H bond insertion accounted for the observed high activity while minimizing the occurrence of *β*-H elimination, leading to alkene byproducts or downstream dual N−H bond insertion. The promising preparation method and favorable catalytic outcomes underscore the potential application of heterogeneous single-atom site catalysts in various organic transformations.

ASSOCIATED CONTENT

Supporting Information

The Supporting Information is available free of charge at https://pubs.acs.org/doi/10.1021/acscatal.3c05635.

Experimental procedures and spectral data for all new products (PDF)

AUTHOR INFORMATION

Corresponding Authors

Dingsheng Wang − *Department of Chemistry, Tsinghua University, Beijing 100084, China;* orcid.org/0000-0003-0074-7633; Email: wangdingsheng@mail.tsinghua.edu.cn

Yadong Li − *Department of Chemistry, Tsinghua University, Beijing 100084, China;* orcid.org/0000-0003-1544-1127; Email: ydli@mail.tsinghua.edu.cn

Jie Zhao − *Key Laboratory for Advanced Materials and Joint International Research Laboratory of Precision Chemistry and Molecular Engineering, Feringa Nobel Prize Scientist*

https://doi.org/10.1021/acscatal.3c05635
ACS Catal. 2024, 14, 4690−4698

Joint Research Center, Frontiers Science Center for Materiobiology and Dynamic Chemistry, School of Chemistry and Molecular Engineering, East China University of Science and Technology, Shanghai 200237, China; Key Laboratory of Bioorganic Phosphorus Chemistry and Chemical Biology (Ministry of Education), Department of Chemistry, Tsinghua University, Beijing 100084, China; orcid.org/0000-0002-0451-0919; Email: zhaojie@ecust.edu.cn

Authors

Ping Guo − *Key Laboratory for Advanced Materials and Joint International Research Laboratory of Precision Chemistry and Molecular Engineering, Feringa Nobel Prize Scientist Joint Research Center, Frontiers Science Center for Materiobiology and Dynamic Chemistry, School of Chemistry and Molecular Engineering, East China University of Science and Technology, Shanghai 200237, China*

Yan Chen − *Key Laboratory for Advanced Materials and Joint International Research Laboratory of Precision Chemistry and Molecular Engineering, Feringa Nobel Prize Scientist Joint Research Center, Frontiers Science Center for Materiobiology and Dynamic Chemistry, School of Chemistry and Molecular Engineering, East China University of Science and Technology, Shanghai 200237, China*

Lei Tao − *University of Chinese Academy of Sciences, Beijing 100049, China*

Shufang Ji − *Department of Chemistry, Tsinghua University, Beijing 100084, China; Department of Chemistry, University of Toronto, Toronto, Ontario M5S 3H6, Canada*

Ruixue Zhang − *Key Laboratory for Advanced Materials and Joint International Research Laboratory of Precision Chemistry and Molecular Engineering, Feringa Nobel Prize Scientist Joint Research Center, Frontiers Science Center for Materiobiology and Dynamic Chemistry, School of Chemistry and Molecular Engineering, East China University of Science and Technology, Shanghai 200237, China*

Zedong Zhang − *Department of Chemistry, Tsinghua University, Beijing 100084, China*

Xiao Liang − *Department of Chemistry, Tsinghua University, Beijing 100084, China*

Complete contact information is available at: https://pubs.acs.org/10.1021/acscatal.3c05635

Author Contributions

#P.G., Y.C., L.T., and S.F. contributed equally to this work. J.Z., D.W., and Y.L. conceived and directed the project; P.G., Y.C., and R.Z. carried out the experiments of catalysis under the guidance of J.Z., L.T. accomplished the DFT studies; S.J. prepared the heterogeneous catalyst and performed the characterizations of catalysts; Z.Z. analyzed the XAFS data; and X.L. carried out the XPS test and collected the XAFS spectra. This manuscript was written through the contributions of all authors.

Notes

The authors declare no competing financial interest.

ACKNOWLEDGMENTS

J.Z. acknowledges the project supported by the Shanghai Municipal Science and Technology Major Project (2018SHZDZX03), the Program of Introducing Talents of Discipline to Universities (B16017), and the National Natural Science Foundation of China (22301076). Y.L. acknowledges the project supported by the NSFC Center for Single-Atom Catalysis (22388102).

REFERENCES

(1) Witham, C. A.; Huang, W.; Tsung, C. K.; Kuhn, J. N.; Somorjai, G. A.; Toste, F. D. Converting homogeneous to heerogeneous in electrophilic catalysis using monodisperse metal nanoparticles. *Nat. Chem.* **2010**, *2* (1), 36−41.

(2) Ye, R.; Zhukhovitskiy, A. V.; Kazantsev, R. V.; Fakra, S. C.; Wickemeyer, B. B.; Toste, F. D.; Somorjai, G. A. Supported Au nanoparticles with N-heterocyclic carbene ligands as active and stable heterogeneous catalysts for lactonization. *J. Am. Chem. Soc.* **2018**, *140* (11), 4144−4149.

(3) Koy, M.; Bellotti, P.; Das, M.; Glorius, F. N-heterocyclic carbenes as tunable ligands for catalytic metal surfaces. *Nat. Catal.* **2021**, *4* (5), 352−363.

(4) Yasukawa, T.; Miyamura, H.; Kobayashi, S. Chiral rhodium nanoparticle-catalyzed asymmetric arylation reactions. *Acc. Chem. Res.* **2020**, *53* (12), 2950−2963.

(5) Yasukawa, T.; Miyamura, H.; Kobayashi, S. Chiral metal nanoparticle-catalyzed asymmetric C-C bond formation re-actions. *Chem. Soc. Rev.* **2014**, *43* (5), 1450−1461.

(6) Qu, R.; Junge, K.; Beller, M. Hydrogenation of carboxylic acids, esters, and related compounds over heterogeneous catalysts: a step toward sustainable and carbon-neutral processes. *Chem. Rev.* **2023**, *123* (3), 1103−1165.

(7) Li, W.; Rabeah, J.; Bourriquen, F.; Yang, D.; Kreyenschulte, C.; Rockstroh, N.; Lund, H.; Bartling, S.; Surkus, A. E.; Junge, K.; Bruckner, A.; Lei, A.; Beller, M. Scalable and se-lective deuteration of (hetero)arenes. *Nat. Chem.* **2022**, *14* (3), 334−341.

(8) Zhang, R.; Chen, Y.; Ding, M.; Zhao, J. Heterogeneous Cu catalyst in organic transformations. *Nano Res.* **2022**, *15* (4), 2810−2833.

(9) Chen, Z.; Vorobyeva, E.; Mitchell, S.; Fako, E.; Ortuno, M. A.; Lopez, N.; Collins, S. M.; Midgley, P. A.; Richard, S.; Vile, G.; Perez-Ramirez, J. A heterogeneous single-atom palladium catalyst surpassing homogeneous systems for Suzuki coupling. *Nat. Nanotechnol.* **2018**, *13* (8), 702−707.

(10) Handa, S.; Wang, Y.; Gallou, F.; Lipshutz, B. H. Sustainable Fe-ppm Pd nanoparticle catalysis of Suzuki-Miyaura cross-couplings in water. *Science* **2015**, *349* (6252), 1087−1091.

(11) Costa, P.; Sandrin, D.; Scaiano, J. C. Real-time fluorescence imaging of a heterogeneously catalysed Suzuki-Miyaura reaction. *Nat. Catal.* **2020**, *3* (5), 427−437.

(12) Sun, B.; Ning, L.; Zeng, H. C. Confirmation of Suzuki-Miyaura cross-coupling reaction mechanism through syn-thetic architecture of nanocatalysts. *J. Am. Chem. Soc.* **2020**, *142* (32), 13823−13832.

(13) Rodriguez, J.; Conley, M. P. A heterogeneous iridium cata-lyst for the hydroboration of pyridines. *Org. Lett.* **2022**, *24* (25), 4680−4683.

(14) Liu, Y.; Wu, X.; Li, Z.; Zhang, J.; Liu, S. X.; Liu, S.; Gu, L.; Zheng, L. R.; Li, J.; Wang, D.; Li, Y. Fabricating polyoxo-metalates-stabilized single-atom site catalysts in confined space with enhanced activity for alkynes diboration. *Nat. Commun.* **2021**, *12* (1), No. 4205.

(15) Xu, Q.; Guo, C.; Li, B.; Zhang, Z.; Qiu, Y.; Tian, S.; Zheng, L.; Gu, L.; Yan, W.; Wang, D.; Zhang, J. Al^{3+} dopants induced Mg2+ vacancies stabilizing single-atom Cu catalyst for efficient free-radical hydrophosphinylation of alkenes. *J. Am. Chem. Soc.* **2022**, *144* (10), 4321−4326.

(16) Miura, H.; Hachiya, Y.; Nishio, H.; Fukuta, Y.; Toyomasu, T.; Kobayashi, K.; Masaki, Y.; Shishido, T. Practical synthesis of allyl, allenyl, and benzyl boronates through SN_1'-type borylation under heterogeneous gold catalysis. *ACS Catal.* **2021**, *11* (2), 758−766.

(17) Liu, B.; Wang, Y.; Huang, N.; Lan, X.; Xie, Z.; Chen, J. G.; Wang, T. Heterogeneous hydroformylation of alkenes by Rh-based catalysts. *Chem.* **2022**, *8* (10), 2630−2658.

(18) Färber, C.; Stegner, P.; Zenneck, U.; Knupfer, C.; Bendt, G.; Schulz, S.; Harder, S. Teaming up main group metals with metallic

iron to boost hydrogenation catalysis. *Nat. Commun.* **2022**, *13* (1), No. 3210.
(19) Liu, F.; Xia, Y.; Xu, W.; Cao, L.; Guan, Q.; Gu, Q.; Yang, B.; Lu, J. Integration of bimetallic electronic synergy with ox-ide site isolation improves the selective hydrogenation of acetylene. *Angew. Chem., Int. Ed.* **2021**, *60* (35), 19324−19330.
(20) Masuda, R.; Yasukawa, T.; Yamashita, Y.; Maki, T.; Yoshida, T.; Kobayashi, S. Heterogeneous single-atom zinc on nitrogen-doped carbon catalyzed electrochemical allylation of imines. *J. Am. Chem. Soc.* **2023**, *145* (22), 11939−11944.
(21) Kita, Y.; Kuwabara, M.; Kamata, K.; Hara, M. Heterogeneous low-valent Mn catalysts for α-alkylation of ketones with alcohols through borrowing hydrogen methodology. *ACS Catal.* **2022**, *12* (19), 11767−11775.
(22) Sun, J. L.; Ci, C.; Jiang, H.; Dixneuf, P. H.; Zhang, M. Utilizing nitroarenes and HCHO to directly construct functional N-heterocycles by supported cobalt/amino acid re-lay catalysis. *Angew. Chem., Int. Ed.* **2023**, *62* (22), No. e202303007.
(23) Xue, W.; Zhu, Z.; Chen, S.; You, B.; Tang, C. Atomically dispersed Co-N/C catalyst for divergent synthesis of nitrogen-containing compounds from alkenes. *J. Am. Chem. Soc.* **2023**, *145* (7), 4142−4149.
(24) Liu, L.; Corma, A. Isolated metal atoms and clusters for alkane activation: translating knowledge from enzymatic and homogeneous to heterogeneous systems. *Chem* **2021**, *7* (9), 2347−2384.
(25) Zhang, B.; Guo, T.; Liu, Y.; Kuhn, F. E.; Wang, C.; Zhao, Z. K.; Xiao, J.; Li, C.; Zhang, T. Sustainable production of benzylamines from lignin. *Angew. Chem., Int. Ed.* **2021**, *60* (38), 20666−20671.
(26) Zhou, B.; Chandrashekhar, V. G.; Ma, Z.; Kreyenschulte, C.; Bartling, S.; Lund, H.; Beller, M.; Jagadeesh, R. V. Development of a general and selective nanostructured cobalt catalyst for the hydrogenation of benzofurans, indoles and benzothiophenes. *Angew. Chem., Int. Ed.* **2023**, *62* (10), No. e202215699.
(27) Sun, K.; Shan, H.; Ma, R.; Wang, P.; Neumann, H.; Lu, G. P.; Beller, M. Catalytic oxidative dehydrogenation of N-heterocycles with nitrogen/phosphorus co-doped porous carbon materials. *Chem. Sci.* **2022**, *13* (23), 6865−6872.
(28) Chandrashekhar, V. G.; Senthamarai, T.; Kadam, R. G.; Malina, O.; Kašlík, J.; Zbořil, R.; Gawande, M. B.; Jagadeesh, R. V.; Beller, M. Silica-supported Fe/Fe-O nanoparticles for the catalytic hydrogenation of nitriles to amines in the presence of aluminium additives. *Nat. Catal.* **2022**, *5* (1), 20−29.
(29) Guo, Y.; Wang, M.; Zhu, Q.; Xiao, D.; Ma, D. Ensemble effect for single-atom, small cluster and nanoparticle catalysts. *Nat. Catal.* **2022**, *5* (9), 766−776.
(30) Wang, A.; Li, J.; Zhang, T. Heterogeneous single-atom catalysis. *Nat. Rev. Chem.* **2018**, *2* (6), 65−81.
(31) Wang, Y.; Mao, J.; Meng, X.; Yu, L.; Deng, D.; Bao, X. Catalysis with two-dimensional materials confining single atoms: concept, design, and applications. *Chem. Rev.* **2019**, *119* (3), 1806−1854.
(32) Kaiser, S. K.; Chen, Z.; Faust Akl, D.; Mitchell, S.; Perez-Ramirez, J. Single-atom catalysts across the periodic table. *Chem. Rev.* **2020**, *120* (21), 11703−11809.
(33) Guo, P.; Liu, H.; Zhao, J. Transforming bulk alkenes and alkynes into fine chemicals enabled by single-atom site catalysis. *Nano Res.* **2022**, *15* (9), 7840−7860.
(34) Li, W. H.; Ye, B. C.; Yang, J.; Wang, Y.; Yang, C. J.; Pan, Y. M.; Tang, H. T.; Wang, D.; Li, Y. A Single-Atom Cobalt Catalyst for the Fluorination of Acyl Chlorides at Parts-per-Million Catalyst Loading. *Angew. Chem., Int. Ed.* **2022**, *61* (40), No. e202209749.
(35) Gan, T.; Wang, D. Atomically dispersed materials: Ideal catalysts in atomic era. *Nano Res.* **2024**, *17*, 18.
(36) Wang, L.; Wu, J.; Wang, S.; et al. The reformation of catalyst: From a trial-and-error synthesis to rational design. *Nano Res.* **2023**, 3261−3301, DOI: 10.1007/s12274-023-6037-8.
(37) Li, W.-H.; Yang, J.; Wang, D.; Li, Y. Striding the threshold of an atom era of organic synthesis by single-atom catalysis. *Chem.* **2022**, *8* (1), 119−140.
(38) Cui, X.; Li, W.; Ryabchuk, P.; Junge, K.; Beller, M. Bridging homogeneous and heterogeneous catalysis by heterogeneous single-metal-site catalysts. *Nat. Catal.* **2018**, *1* (6), 385−397.
(39) Li, W. H.; Yang, J.; Jing, H.; Zhang, J.; Wang, Y.; Li, J.; Zhao, J.; Wang, D.; Li, Y. Creating High Regioselectivity by Electronic Metal-Support Interaction of a Single-Atomic-Site Catalyst. *J. Am. Chem. Soc.* **2021**, *143* (37), 15453−15461.
(40) Zhang, J.; Wang, Z. Y.; Chen, W. X.; Xiong, Y.; Cheong, W. C.; Zheng, L. R.; Yan, W. S.; Gu, L.; Chen, C.; Peng, Q.; Hu, P.; Wang, D.; Li, Y. Tuning polarity of CuO bond in heterogeneous Cu catalyst to promote additive-free hydroboration of alkynes. *Chem* **2020**, *6*, 725−737, DOI: 10.1016/j.chempr.2019.12.021.
(41) Wang, J.; Che, C.; Doyke, M. P. *Transition Metal-catalyzed Carbene Transformations*; Wiley-VCH GmbH Press, 2022.
(42) Liu, Z.; Yang, Y.; Song, Q.; Li, L.; Zanoni, G.; Liu, S.; Xiang, M.; Anderson, E. A.; Bi, X. Chemoselective carbene insertion into the N-H bonds of NH3·H2O. *Nat. Commun.* **2022**, *13* (1), No. 7649.
(43) Liu, Z.; Calvo-Tusell, C.; Zhou, A. Z.; Chen, K.; Garcia-Borras, M.; Arnold, F. H. Dual-function enzyme catalysis for enantioselective carbon-nitrogen bond formation. *Nat. Chem.* **2021**, *13* (12), 1166−1172.
(44) Dai, L.; Chen, Y. Y.; Xiao, L. J.; Zhou, Q. L. Intermolecular enantioselective benzylic C(sp3)-H amination by cationic copper catalysis. *Angew. Chem., Int. Ed.* **2023**, *62* (24), No. e202304427.
(45) Li, M.-L.; Pan, J.-B.; Zhou, Q.-L. Enantioselective synthesis of amino acids from ammonia. *Nat. Catal.* **2022**, *5* (6), 571−577.
(46) Pan, J. B.; Zhang, X. G.; Shi, Y. F.; Han, A. C.; Chen, Y. J.; Ouyang, J.; Li, M. L.; Zhou, Q. L. A spiro phosphamide catalyzed enantioselective proton transfer of ylides in a free carbene insertion into N-H bonds. *Angew. Chem., Int. Ed.* **2023**, *62* (15), No. e202300691.
(47) Ma, C.; Wang, S.; Sheng, Y.; Zhao, X.-L.; Xing, D.; Hu, W. Synthesis and characterization of donor-acceptor iron porphyrin carbenes and their reactivities in N-H insertion and related three-component reaction. *J. Am. Chem. Soc.* **2023**, *145* (9), 4934−4939.
(48) Steck, V.; Carminati, D. M.; Johnson, N. R.; Fasan, R. Enantioselective synthesis of chiral amines via biocatalytic carbene N-H insertion. *ACS Catal.* **2020**, *10* (19), 10967−10977.
(49) Wang, K.; Liu, Z.; Xu, G.; Shao, Y.; Tang, S.; Chen, P.; Zhang, X.; Sun, J. Chemo- and enantioselective insertion of furyl carbene into the N-H bond of 2-pyridones. *Angew. Chem., Int. Ed.* **2021**, *60* (31), 16942−16946.
(50) Gutiérrez, S.; Tomas-Gamasa, M.; Mascarenas, J. L. Exporting metal-carbene chemistry to live mammalian cells: copper-catalyzed intracellular synthesis of quinoxalines enabled by N-H carbene insertions. *Angew. Chem., Int. Ed.* **2021**, *60* (40), 22017−22025.
(51) Li, W.; Wang, J.; Hu, X.; Shen, K.; Wang, W.; Chu, Y.; Lin, L.; Liu, X.; Feng, X. Catalytic asymmetric roskamp reaction of α-alkyl-α-diazoesters with aromatic aldehydes: highly enantioselective synthesis of α-alkyl-β-keto esters. *J. Am. Chem. Soc.* **2010**, *132* (25), 8532−8533.
(52) Tan, F.; Pu, M.; He, J.; Li, J.; Yang, J.; Dong, S.; Liu, X.; Wu, Y.-D.; Feng, X. Catalytic asymmetric homologation of ketones with α-alkyl α-diazo esters. *J. Am. Chem. Soc.* **2021**, *143* (5), 2394−2402.
(53) Dong, S.; Liu, X.; Feng, X. Asymmetric Catalytic Rearrangements with α-Diazocarbonyl Compounds. *Acc. Chem. Res.* **2022**, *55* (3), 415−428.
(54) Li, S.; Zhang, C.; Pan, G.; Yang, L.; Su, Z.; Feng, X.; Liu, X. Enantioselective Photochemical Carbene Insertion into C-C and C-H Bonds of 1,3-Diketones by a Guanidine-Amide Organocatalyst. *ACS Catal.* **2023**, *13* (7), 4656−4666.
(55) DeAngelis, A.; Panish, R.; Fox, J. M. Rh-catalyzed intermolecular reactions of α-alkyl-α-diazo carbonyl compounds with selectivity over β-hydride migration. *Acc. Chem. Res.* **2016**, *49* (1), 115−127.
(56) DeAngelis, A.; Dmitrenko, O.; Yap, G. P. A.; Fox, J. M. Chiral crown conformation of Rh2(S-PTTL)4: enantioselective cyclopropanation with α-alkyl-α-diazoesters. *J. Am. Chem. Soc.* **2009**, *131* (21), 7230−7231.

https://doi.org/10.1021/acscatal.3c05635
ACS Catal. 2024, 14, 4690−4698

(57) Li, M.-L.; Yu, J.-H.; Li, Y.-H.; Zhu, S.-F.; Zhou, Q.-L. Highly enantioselective carbene insertion into N-H bonds of aliphatic amines. *Science* **2019**, *366* (6468), 990−994.
(58) Li, Y.; Zhao, Y.-T.; Zhou, T.; Chen, M.-Q.; Li, Y.-P.; Huang, M.-Y.; Xu, Z.-C.; Zhu, S.-F.; Zhou, Q.-L. Highly enantioselective O-H bond insertion reaction of α-alkyl- and α-alkenyl-α-diazoacetates with water. *J. Am. Chem. Soc.* **2020**, *142* (23), 10557−10566.
(59) Yu, Z.; Li, Y.; Shi, J.; Ma, B.; Liu, L.; Zhang, J. (C6F5)3B catalyzed chemoselective and ortho-selective substitution of phenols with α-aryl α-diazoesters. *Angew. Chem., Int. Ed.* **2016**, *55* (47), 14807−14811.
(60) Zhao, J.; Ji, S.; Guo, C.; Li, H.; Dong, J.; Guo, P.; Wang, D.; Li, Y.; Toste, F. D. A heterogeneous iridium single-atom-site catalyst for highly regioselective carbenoid O-H bond insertion. *Nat. Catal.* **2021**, *4* (6), 523−531.

https://doi.org/10.1021/acscatal.3c05635
ACS Catal. 2024, 14, 4690−4698